

# Autonomous Waypoint-based Guidance Methods for Small Size Unmanned Aerial Vehicles

**Dániel Stojcsics**

Óbuda University, John von Neumann Faculty of Informatics, Budapest, Hungary  
stojcsics.daniel@nik.uni-obuda.hu

---

*Abstract: The AERObot is a special ARM microcontroller-based autopilot for small and medium size UAVs<sup>1</sup> developed at Óbuda University for research purposes. The aim of the research was to create a generic autopilot which is capable of controlling different design, weight and structure airframes without any complex parameter or model recalculation as usual for e.g. switching between tailless or classic tail aircrafts. For this purpose a simple, desired heading-based guidance method was developed which is easy to visualize and needs only a few parameters to be set while the quality remains the same as the existing ones. The paper presents a new guidance method and a few example controller types which can fit it. Test flights were made to demonstrate the real time operation and low computation needs of the presented methods.*

*Keywords: Unmanned Aerial Vehicle; UAV; Guidance; Navigation; Fuzzy; Mamdani Controller; Nonlinear Controller*

---

## 1 Introduction

Most of the UAV autopilots are based on a complex mathematical model using differential equations of motion. These approaches are perfect for most controller types such as classical control [1, 2, 3, 4, 5], state-space methods [6], optimal or robust control [7] and even for fuzzy control [8, 9] system. The problem with those approaches are their strong model based behaviour. These systems are sensitive of the model changes e.g. electric to glow engine conversion or different airframe structures (classic or tailless). With this approach a specific autopilot cannot control these airframes without strong modification of the used model reference and control system approach.

---

<sup>1</sup> Unmanned Aerial Vehicle

Instead of the previous approach AERObot is using and RC<sup>2</sup> based solution even with multiple navigation and control methods. Most of the RC modellers are using the same quasi-standard four basic channel based transmitter to control model planes from small to large size (under 1 kg to 10+ kg). With these basic channels (aileron, elevator, rudder and throttle) they can control the model in all three axes (lateral, longitudinal and vertical) with proper thrust control. This approach is independent from the plane structural design (easy driveable classic trainer, a gentle glider, a special tailless plane or even a high speed jet). The main difference of these is the inertia. The smaller plane is more agile. This behaviour is easy to handle with the end point adjustment of the actuators (limiting the turn rates).

For the small size UAVs (under 10 kg) the structural deformations, aeroelastic behaviour of the wing can be neglected since the used materials (fiberglass, carbon parts as reinforcement or even complete composite structures) for the airframe can handle more than 10 times more force than the larger, heavier ones because of their structural design and high strength to weight ratio [10].

With such an approach AERObot is capable of fully autonomous flight with real time onboard guidance, navigation and control with a on-board ARM-based embedded microcontroller unit. The core (STM32F103) is running at 72MHz clock speed, capable of up to 90 MIPS only but it is lightweight which makes the device ideal for small size aerial applications.

The current paper presents the complete simulation and real flight testing of the created guidance method in order to demonstrate the real time application and practical applicability of the system. The paper is structured as follows: section 2 presents the simulation possibilities. Sections 3 and 4 describe the estimations needed for the guidance presented in section 5. Then sections 6 and 7 presents the simulated and real test flight results, summarized in the conclusions finally. The extended version of the presented methods can be found on [11].

## 2 The HIL Simulation

The Aerosim blockset Matlab provides a complete solution for guidance, navigation and control of an unmanned aerial vehicle under Matlab. A general 6 DoF nonlinear UAV model with all the equations of motion is provided in the blockset for further research, e.g. custom UAV identification [12].

The 6 DoF system is using an atmosphere and earth model for the computation of the aerodynamics, propulsion, and inertia model, used for the equations of motion (Fig. 1), fully described in [13], calculating the momentum, acceleration, orientation, position etc of the unmanned aircraft. The HIL simulation is able to

---

<sup>2</sup> Radio Control

create the same environment as the real flight. The autopilot is acting the same as real; it has no information about the source of the measured signals which are generated with PC simulation software. A mathematical model created in Matlab/Simulink (Fig. 2) processes the states of the UAV using the actuator signals captured from the autopilot [14]. The autopilot is using the simulated signals instead of its own internal sensors for the filter, navigation and control algorithms. The simulator sends the output of the simulation (position, orientation, airspeed and altitude etc.) to the autopilot via serial port with a desired control frequency (e.g. 100 Hz) which is the same as the update frequency of the control functions (discrete time simulation with a real time model). The autopilot is not using its internal timer but the timestamp from the simulator.

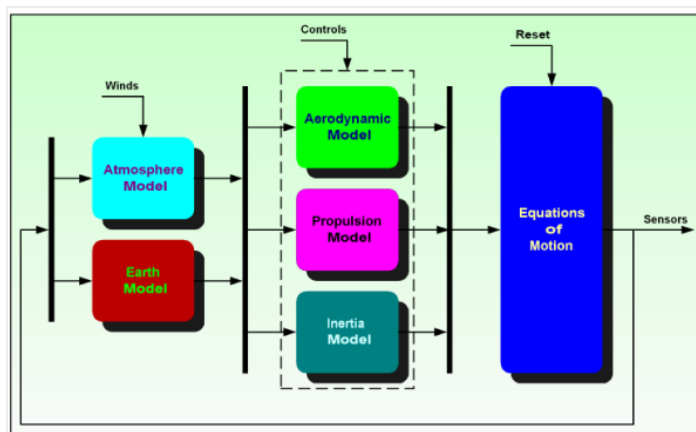


Figure 1

6-DoF unmanned aircraft dynamics system: Aerosim

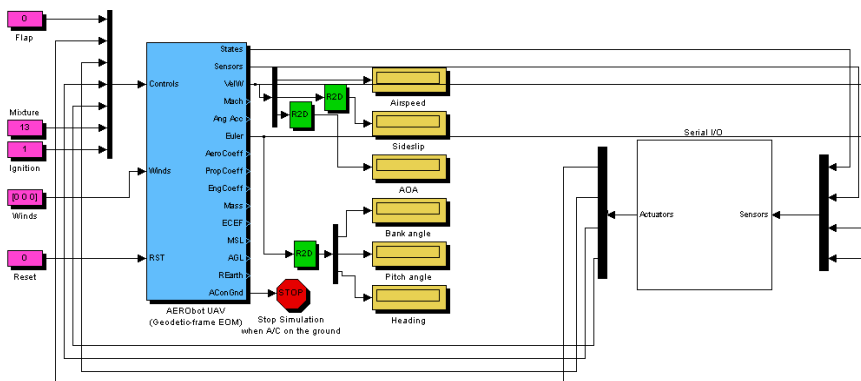


Figure 2

Matlab HIL model using Simulink and AeroSim blockset with serial i/o

The generic small size fixed wing UAV model was created in Matlab/Simulink using the AeroSim block set using a predefined UAV 6 DoF<sup>3</sup> model for the validation purposes of the HIL simulation [14]. A lot of conclusion and test data are available for the control functions and navigation from real flights in the past [11], so the simulated results could be compared to real measured ones. The selected block set has an interface to FlightGear flight simulator so the HIL test flights can be observed in such a graphical way. The simulated outputs can be ideal or noisy (generated). Using ideal values the internal filters can be bypassed. Otherwise the HIL simulation is capable of testing the onboard software filters in different situations. The autopilot calculates and sends back the actuator signals based on the received values while also refreshing the physical actuator. These signals are the inputs of the simulation model.

### 3 Bearing Estimation

The base sensor for the navigation is the GPS<sup>4</sup>. It provides the position, SOG<sup>5</sup>, bearing and many other parameters used by the navigation algorithms. The maximum position refresh rate of best GPS modules is about 5-10 Hz, which is not enough for precision flight control.

The other problem is that the refresh rate is not reliable because NMEA<sup>6</sup> sentences and the checksums are often incorrect. It is necessary to estimate the missing, and intermediate positions for the continuous bearing control (100 Hz – update frequency of the most actuators). This estimation can be computed using the vertical angular velocity and the GPS bearing from the last valid NMEA sentence. The actual bearing can be estimated between two valid GPS sentences (1), fully described in [11]. The heading angle provided by the IMU is often not reliable, because of the magnetic sensor used by the internal sensor fusion algorithms. This sensor is very sensitive to strong electromagnetic fields especially when the UAV has electric propulsion.

$$\theta_e = \theta + \dot{\psi}t_s \quad (1)$$

where:

- $\theta$ : previous bearing (measured by GPS)
- $\theta_e$ : estimated bearing
- $\dot{\psi}$ : angular velocity
- $t_s$ : sample time

---

<sup>3</sup> Degrees of freedom

<sup>4</sup> Global Positioning System

<sup>5</sup> Speed over ground

<sup>6</sup> National Marine Educators Association – Predefined sentence types used by GPS modules

Small size (around 1 m wingspan) and small weight (under 2 kg) UAVs are quite agile so turn rates can reach high levels. For these airframes bearing estimation is essential (Fig. 3), details presented in [15].



Figure 3

Xeno UAV flight test, purple triangle indicates the estimated bearing (circles marks the waypoints)

## 4 Position Estimation

During the navigation, not only the bearing but also the position has to be estimated with a navigation formula given in (2) well known in nautical terms [16]. The aim is not a complete inertial navigation system with the minimal error but to compute intermediate positions and bearing to achieve better performance so some things like local airflow parameters or slideslip angle can be ignored [17, 18, 19, 20].

$$Lat_2 = \text{asin}(\sin(Lat_1) * \cos\left(\frac{d}{R}\right) + \cos(Lat_1) * \sin\left(\frac{d}{R}\right) * \cos(\theta_e))$$

$$Lon_2 = Lon_1 + \text{atan2}(\sin(\theta_e) * \sin\left(\frac{d}{R}\right) * \cos(Lat_1), \cos\left(\frac{d}{R}\right) - \sin(Lat_1) * \sin(Lat_2))$$

where:

- $Lat_1$ : previous estimated latitude of the UAV
- $Lon_1$ : previous estimated longitude of the UAV
- $\theta_e$ : estimated bearing (in radians, clockwise from north);
- $d$ : travelled distance
- $R$ : Earth radius

Usually there are 200 ms between two valid GPS sentence burst [21], but the distribution of measured positions are not uniform. Even if one or two is corrupted the refresh time is always under 1000 ms. Because of this, the direction and

velocity of the wind can be ignored. During the estimation the last known SOG can be used no matter how the bearing of the UAV changed (compared to the wind). Obviously there will be some estimation errors, but usually it is low (under 1 m) and not causing any serious false position estimation [15].

The estimation (Fig. 4) can be calculated from the previous known SOG, estimated position and bearing (when known position and bearing are not available) [11].

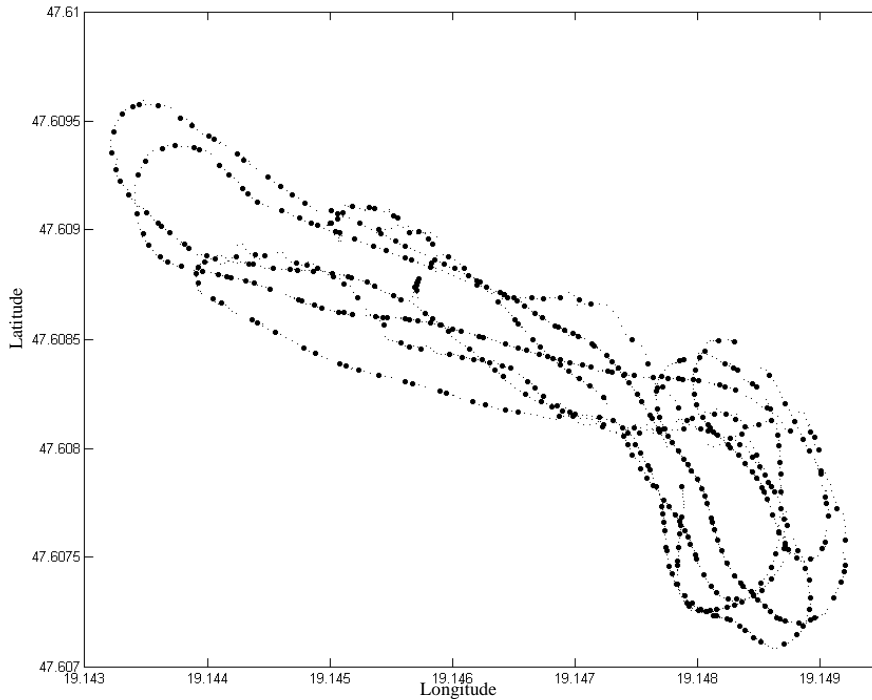


Figure 4

Position estimation simulation from telemetry data  
(downsampled, big dots are the measured, small dots are the estimated positions)

## 5 Guidance

There are many guidance approaches. Most of them are using waypoints [22], defined by a geographic position (latitude and longitude), an altitude (AGL<sup>7</sup> or ASL<sup>8</sup>) and a waypoint radius (usually 25-75 m, used to achieve precise path tracking). A waypoint is reached, when the distance between the UAV and the waypoint is under the predefined radius value.

### 5.1 Guidance using Bearing and Cross Track Error

The easiest way to navigate between waypoints is a basic navigation used by the most nautical and handheld GPS devices such as the Garmin eTrex [23]. The bearing and position of the UAV is given, the cross track error ( $l$ ), waypoint bearing ( $\alpha$ ) and the bearing – path angle difference ( $\beta$ ) can be calculated (Fig. 5). For this navigation a special third order non-linear controller was created using the error values ( $\alpha, \beta, l$ ). The aim of the created controller [24] is to minimize the error of the presented triplet. The third order was obtained by a special transfer function introduced in [14] and tuned based on our measurements in [11].

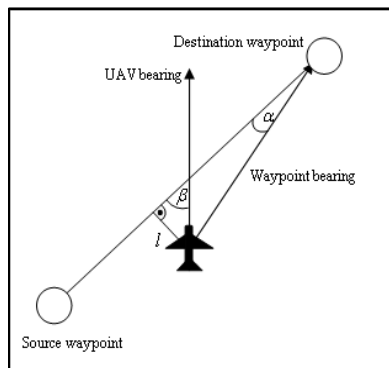


Figure 5

Navigation scheme using bearing and cross track error

### 5.2 Vector Field Guidance

The new vector field guidance calculates a desired bearing in every position, no matter what is the actual bearing of the UAV based on the same input sensor data as the “classic guidance” using bearing and cross track error.

<sup>7</sup> Above ground level

<sup>8</sup> Above sea level

This can be easily represented as a vector field. The desired bearing depends on the position of the UAV, source and destination waypoints and the cross track error [11]:

$$\delta = \sqrt[k_d]{|D_{CT} * K_c * (\varphi_T - \varphi_R)|} * \text{sign}(D_{CT})$$

$$\gamma = \min(1, D_T)$$

$$\varphi_d = \varphi_T + \delta * \gamma \quad (3)$$

where:

- $D_{CT}$ : Cross track error,
- $D_T$ : Distance from target
- $\varphi_d$ : Desired bearing,
- $\varphi_T$ : Bearing from the UAV to the destination waypoint,
- $\varphi_R$ : Bearing from the previous to the destination waypoint,
- $K_d$ : Path reaching gain,
- $K_c$ : Cross track error gain,
- $\gamma$ : Waypoint bearing gain.

The cross track error sensitivity can be set with the  $K_c$  parameter (Fig. 6) and the path reaching smoothness (Fig. 7) with  $K_d$  [11]. It is a common problem that the UAV misses the waypoint if the waypoint radius is low and there is a strong wind or the distance between the source and destination points is short. In this case the UAV should turn back and the flight path will contain unnecessary loops. The first possibility to avoid this problem is the dynamic radius which must suit the local airflow characteristics.

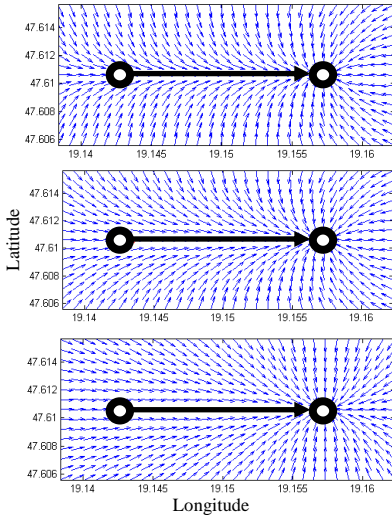


Figure 6

Effect of  $K_c$  with different values (10, 1, 0)

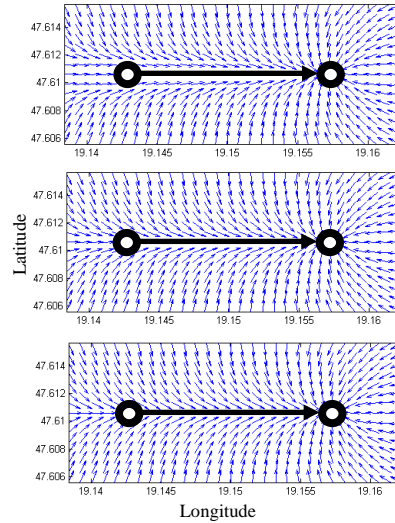


Figure 7

Effect of  $K_d$  with different values (1, 0.5, 0.3)



The other, and better solution is the usage of  $\gamma$ . If the UAV is close to the destination point (under 1000m) the parameter  $\gamma$  guarantees the reach of the waypoint, ignoring  $\delta$  that depends on the UAV – waypoint distance (Fig. 8). This solution was realized by our approach [11].

The first advantage of this navigation is the easy graphical setup of the internal parameters  $K_c$  (~10.0) and  $K_d$  (~0.5). The other is that it has only one output parameter ( $\varphi_d$ ) so nearly any controller type (such as third order non-linear, PID, fuzzy etc.) can fit this navigation because only one value, the difference of desired and actual bearing should be minimized. Furthermore, with a little modification based on (4) [11] it is capable of loiter navigation over a desired position (Fig. 9).

$$\varphi_d = \varphi_T + \frac{\pi}{2} + \min\left(|D_{CT} * K_c|, \frac{\pi}{2}\right) * \text{sign}(D_{CT}) \tag{4}$$

where:

- $D_{CT}$ : Cross track error (distance from the radius),
- $\varphi_d$ : Desired bearing,
- $\varphi_T$ : Bearing from the UAV to the destination waypoint,
- $K_c$ : Cross track error gain.

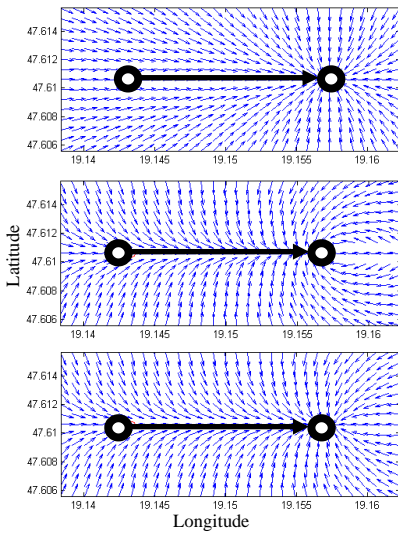


Figure 8

Effect of  $\gamma$  with different values  
(0, 1,  $\min(1, D_T)$ )

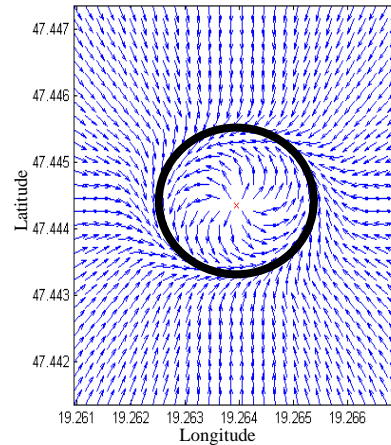


Figure 9  
Loiter navigation

## 6 Controller

There are many things to consider during the selection of an appropriate controller for the UAV. The classic PID controller has many benefits, several autopilots are using it [25, 26, 27, 28]. The setup process of these autopilots is pretty difficult or they can be used with strong limitations, due to the non-linear aircraft characteristics [4, 5].

### 6.1 Third Order Non-Linear Controller

At least three controller channels and a few compensators are needed to control an unmanned airplane and achieve the appropriate flight characteristics. The basic controller channels are the airspeed, altitude and bearing (guidance) [29, 30, 31]. The implementation can be different based on the available flight data. The AERObot autopilot controls the altitude with the engine throttle and the airspeed with the elevator. In case of electric propulsion (continuously decreasing performance because of the electric battery characteristics), this implementation provides adequate airspeed control.

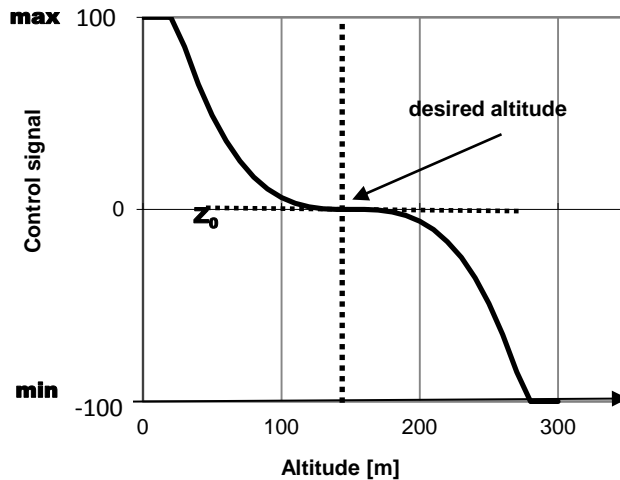


Figure 10

Transfer diagram of the third order non-linear controller

A special non-linear third order controller [32] function has been applied to the AERObot autopilot. The advantage of this is the capability to control non-linear systems like UAVs without linearization. Furthermore several years of practical experience are available for this kind of controller. The transfer functions used in

the controllers can be interpreted as seen on Fig. 10. The target value (i.e.  $X_c=150$  m - altitude controller) and the neutral output for that ( $Z_0=0$ , trim condition) has been marked. If the target altitude is higher than the current measured altitude, the output will be higher than the neutral value. If the target altitude is lower than the current measured altitude, the output will be lower than the neutral value. The function outputs must be limited between predefined values (e.g.  $\pm 100$ ) for practical use. This control method can be used for control surfaces with symmetrical deflection, e.g. the rudder, aileron, elevator or the engine (both electric and glow) throttle. The central “flat” part of the function should be the trim output value ( $Z_0$ ) e.g. the throttle control signal at level flight. This controller is capable of controlling the airspeed, altitude directly and with a little modification it is also suitable for navigation. The navigation controller (5) using the calculated values ( $\alpha$ ,  $\beta$ ,  $l$ ) gives the control signal ( $K_h$ ) which drives directly the rudder (and ailerons) [29].

Detailed analysis was made before the flight test to examine the effect of navigation parameters. Neglecting path tracking sensitivity ( $h_1 = 0$ ) results only the reach of target waypoint but with major cross track error. Increasing this parameter, proper path tracking can be achieved with minimal cross track error.

$$K_h = \begin{cases} \text{if } (((\alpha - \beta) * h_0 + l * (90^\circ + \beta + |\alpha - \beta|) * h_1) * h_2)^3 > \max, \text{ then } \max, \\ \text{if } (((\alpha - \beta) * h_0 + l * (90^\circ + \beta + |\alpha - \beta|) * h_1) * h_2)^3 < \min, \text{ then } \min, \\ \text{else } (((\alpha - \beta) * h_0 + l * (90^\circ + \beta + |\alpha - \beta|) * h_1) * h_2)^3 \end{cases} \quad (5)$$

where

- $K_h$ : control signal of the rudder (neutral = 0),
- $\alpha$ : waypoint direction,
- $\beta$ : bearing – path angle difference,
- $l$ : cross track error,
- $h_0$ : direction sensitivity parameter,
- $h_1$ : path tracking sensitivity parameter,
- $h_2$ : global sensitivity parameter (useful in the real flight tests).

## 6.2 Fuzzy Control

The fuzzy control box was created with the Matlab fuzzy toolbox using Mamdani-type controller. The inputs of the controller box are the same as in the third order controller (target speed, target altitude, actual airspeed, actual altitude, bank angle, pitch angle, heading error). The outputs are the same too (control surface deflection and engine throttle commands).

The fuzzy controller box contains five simple fuzzy controller channels and two linear compensators [33]. There are two stabilization channels (bank and pitch angle) in addition to the three classic controllers (airspeed, altitude, heading). In the case of the third order controller, they were embedded into the three classic

channels. Every controller is a simple Mamdani controller with two (bank angle, pitch angle, heading) or three (airspeed, altitude) triangular input and output membership functions (Fig. 11, 12) with centroid defuzzyfication method [34].

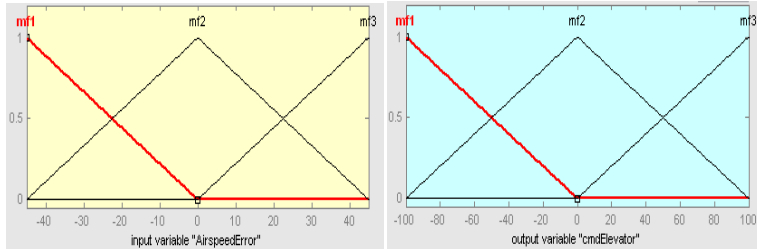


Figure 11

Visual representation of the three triangular input and output membership functions (airspeed controller)

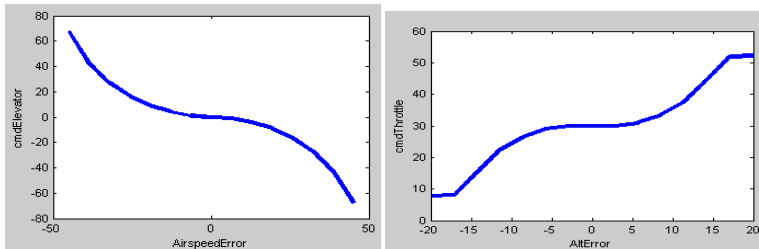


Figure 12

The transfer diagrams of the Mamdani controllers with two (airspeed) and three (altitude) membership functions

In some cases, non-linear compensators must be used which correlates with airspeed or bank angle. Using both pitch and bank angle controllers there is no need for this. The rudder – aileron compensator is needed for the precise navigation. Without this the UAV cannot perform banked turns. The turn radius can be way more than 100 meters instead of the desired 10-20 meters (Fig. 13). The proper value can be specified with HIL simulation flight tests (Fig. 14, 15).

## 7 Test Flights

Many test flights has been made with different size and weight UAVs during the years to test the navigation and the control methods. Test UAVs were based on classic and tailless airframes with both electric and glow propulsion. All the real flights were made after many hours of HIL simulation tests.

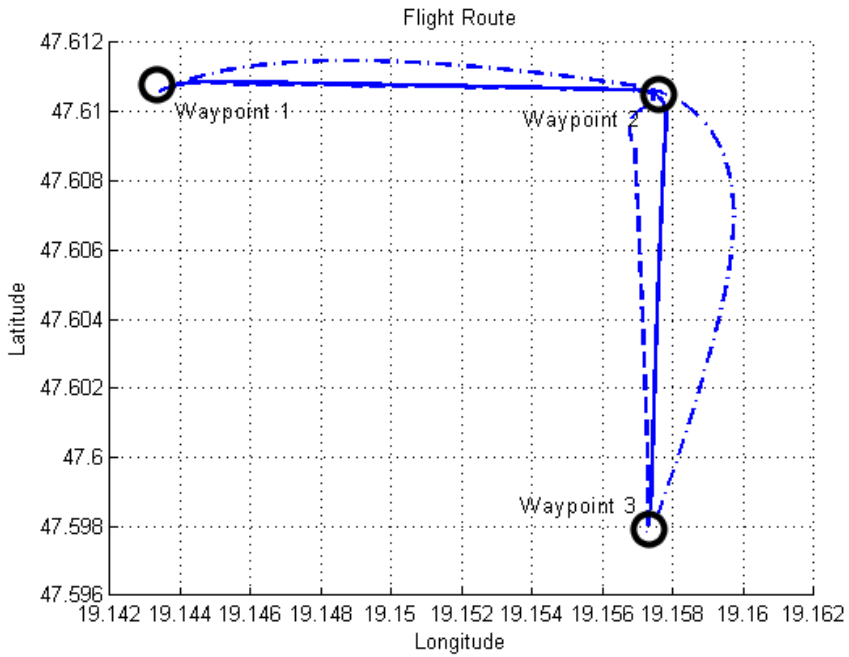


Figure 13

Effect of rudder – aileron compensator with different parameters on the flight route with three waypoints - waypoints marked with circles

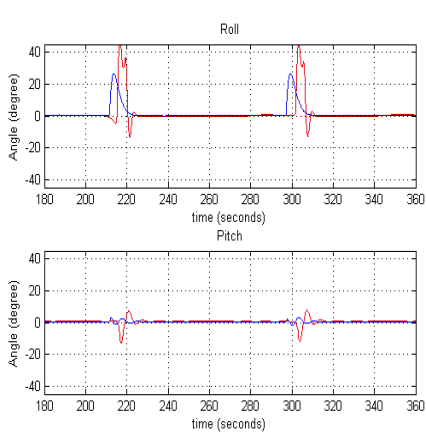


Figure 14

UAV roll and pitch angle plot of two turns  
(blue: fuzzy, red: third order)

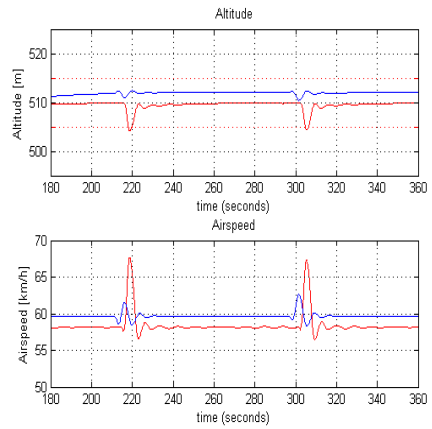


Figure 15

Airspeed and altitude plot of two turns  
(blue: fuzzy, red: third order)

## 7.1 Tiger 60 UAV

The Tiger 60 is a 1.7 m wingspan UAV with classic acrobatic trainer airframe with a 10 cm<sup>3</sup> internal combustion engine [35]. The mass of the plane is 4kg with AERObot autopilot, additional electronics and fuel. It has a built in XBee Pro 2.4 GHz modem for real time telemetry for commands and monitoring flight parameters.

The plane has third order non-linear controllers with bearing and cross track error navigation. The AERObot is capable of manual, autonomous and heterogenous flight. The take-off and landing was made in manual mode, the waypoint flight in autonomous (Fig. 16).

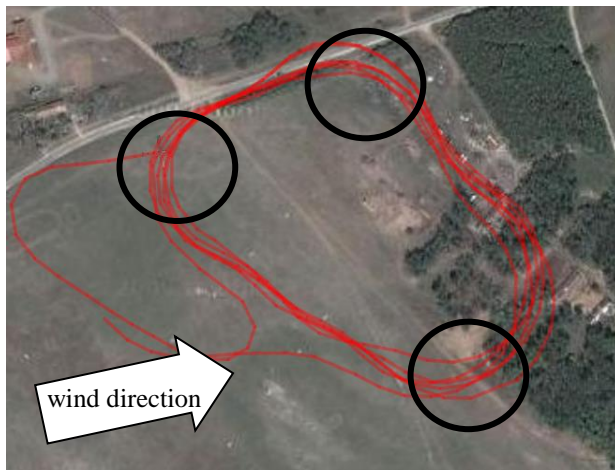


Figure 16

Tiger 60 UAV test flight in a three waypoint continuous route (waypoints marked with circles)

The desired airspeed was 90 km/h and the altitude is 150 m AGL. The routeplan was continuous and contained three waypoints. During the test flight there was a moderate wind which had little influence on the flight path. Both airspeed and altimeter controller had a small offset error (Fig. 17) since the controller has no integrator part.

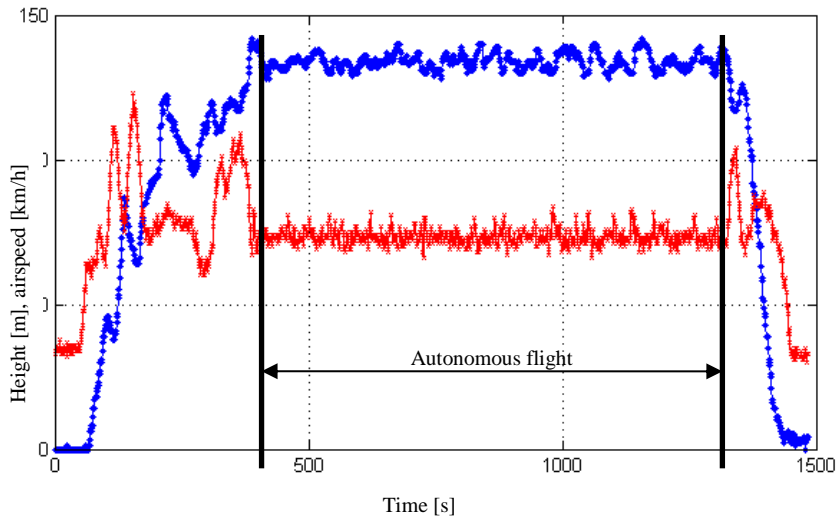


Figure 17

Autonomous flight (red cross: airspeed [km/h], blue dot: height [m])

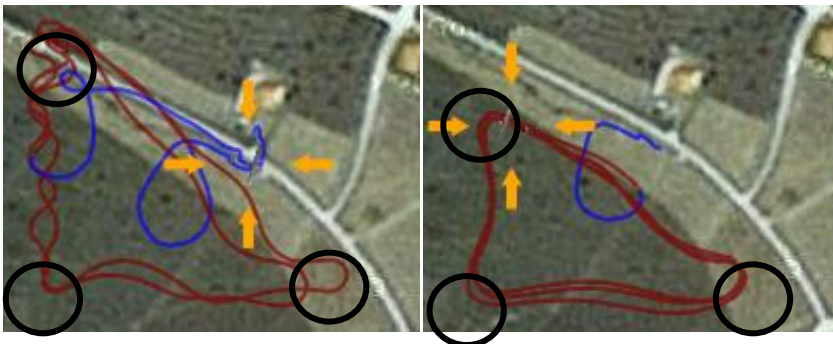


Figure 18

Bearing sensitivity on a continuous three waypoint flight route

(left: without estimation, right: with bearing and position estimation, waypoints marked with circles)

## 7.2 Xeno Tailless UAV

The Xeno is a small size tailless UAV (wingspan: 1.3 m, AUW<sup>9</sup>: 1.2 kg) made from elapor foam [36]. Because of its size and weight it is quite agile and sensitive to the GPS position and bearing errors. Without bearing and position estimations, discussed earlier, it cannot perform precision waypoint flight. It has no direct vertical axis (yaw) control surface since it is a tailless airplane. Vertical

<sup>9</sup> All up weight

axis movements are replaced with longitudinal axis banked turns making the UAV much more sensitive to bearing control than the bigger Tiger 60. The bearing and position estimation algorithms were tested successfully (Fig. 18). The used navigation for this UAV was the previously discussed vector field navigation with PID and Fuzzy controllers.

### **Conclusions**

The discussed vector field navigation method with bearing and position estimation is suitable for any generic autopilot for small size UAVs. As the HIL simulation and the test flights have shown the AERObot with the discussed methods are capable of controlling different design, weight and structure airframes without any complex mathematical model recalculation unlike the other strongly model based autopilots. It has no major sensitivity for the airframe structure, propulsion or any other main dominant factor.

The system has an easy setup interface where the user can set the UAV type, actuator idle and end points as well as the controller gains, like in the case of an RC model and its generic RC transmitter.

AERObot can control not only conventional fixed wing planes but agile special tailless flying wings with low radar cross-section. This feature makes it an ideal platform to develop new navigational, control or stabilizer methods.

As a result a low computation time guidance method was created and successfully tested with multiple on-board real time controller types. Test flights have promising results. Further research is needed for precision guidance and optimal control strategies to achieve low energy consumption and longer flight times.

### **References**

- [1] Y. Shengyi, L. Kunqin, S. Jiao: Optimal Tuning Method of PID Controller Based on Gain Margin and Phase Margin, International Conference on Computational Intelligence and Security, 2009, pp. 634-638, ISBN: 978-1-4244-5411-2
- [2] V. Kargin: Design of an Autonomous Landing Control Algorithm for a Fixed Wing UAV, MS Thesis, Middle East Technical University, Ankara, Turkey, 2007
- [3] J. Amahah: The Design of an Unmanned Aerial Vehicle Based on the ArduPilot, Georgian Electronic Scientific Journal: Computer Science and Telecommunications, 2009, No. 5 (22), pp. 144-153
- [4] Cho et al.: Fully Automatic Taxiing, Takeoff and Landing of a UAV using a Single-Antenna GPS Receiver only, International Conference on Control, Automation and Systems 2007, Oct. 17-20, 2007 in COEX, Seoul, Korea, ISBN: 978-89-950038-6-2, pp. 821-825



- [5] H. Chao, Y. Luo, L. Di and Y. Chen: "Fractional Order Ight Control of Small Fixedwing UAV: Controller Design and Simulation Study", Proceedings of the ASME 2009 International Design Engineering Technical Conferences and Computers and Information in Engineering Conference, 2009, pp. 621-628, ISBN: 978-0-7918-4900-2
- [6] V. V. Patel et al: L1 Adaptive Controller for Tailless Unstable Aircraft, Proceedings of the 2007 American Control Conference, 2007, ISBN: 1-4244-0988-8, pp. 5272-5277
- [7] W. Rui, Z. Zhou and S. Yanhang: Robust Landing Control and Simulation for Flying Wing UAV, Proceedings of the 26<sup>th</sup> Chinese Control Conference, July 26-31, 2007, Zhangjiajie, Hunan, China, ISBN: 978-7-81124-055-9, pp. 600-604
- [8] K. Bickraj, T. Pamphile, A. Yenilmez, M. Li, I. N. Tansel: Fuzzy Logic Based Integrated Controller for Unmanned Aerial Vehicles, Florida Conference on Recent Advances in Robotics, FCRAR 2006
- [9] S. Kurnaz, O. Çetin: Autonomous Navigation and Landing Tasks for Fixed Wing Small Unmanned Aerial Vehicles, Acta Polytechnica Hungarica Vol. 7, No. 1, 2010, pp. 87-102
- [10] D. Cadogan, W. Graham, T. Smith: Inflatable and rigidizable wings for unmanned aerial vehicles, 2<sup>nd</sup> AIAA "Unmanned Unlimited" Systems, Technologies, and Operations, 2003, California, USA
- [11] D. Stojcsics, A. Molnár: AirGuardian – UAV Hardware and Software System for Small Size UAVs, International Journal of Advanced Robotic Systems, 2012, Croatia, ISSN 1729-8806, DOI: 10.5772/52759, Vol. 9, 174:2012, pp. 1-8
- [12] Y. C. Paw, G. J. Balas: Parametric Uncertainty Modeling for LFT Model Realization, 2008 IEEE Int Symposium on Computer-aided Control System Design, USA, September 3-5, 2008
- [13] "AeroSim Blockset User's Guide", Unmanned Dynamics LCC, USA, 2004
- [14] A. Molnár, D. Stojcsics: HIL szimuláció a robotpilóta fejlesztésben, Repüléstudományi Konferencia, Repüléstudományi közlemények különszám, 2011, Szolnok
- [15] D. Stojcsics: Flight Safety Improvements for Small Size Unmanned Aerial Vehicles, IEEE 16<sup>th</sup> International Conference on Intelligent Engineering Systems 2012, Lisbon, Portugal, ISBN: 978-1-4673-2693-3 (pendrive); 978-1-4673-2692-6 (printed), pp. 483-487
- [16] F. Ucan, D.T. Altılar: Navigation and Guidance Planning for Air Vehicles, 20<sup>th</sup> IEEE International Conference on Tools with Artificial Intelligence, ICTAI 2008, Vol. 2, No., pp. 534-538

- [17] Q. Li, Z. Fang, H. Li: The Application of Integrated GPS and Dead Reckoning Positioning in Automotive Intelligent Navigation System, *Journal of Global Positioning Systems* (2004) Vol. 3, No. 1-2: 183-190
- [18] P. Davidson, J. Hautamäki, J. Collin: Using Low-Cost MEMS 3D Accelerometers and One Gyro to Assist GPS-based Car Navigation System, *Proceedings of 15<sup>th</sup> Saint Petersburg International Conference on Integrated Navigation Systems*, May 2008
- [19] L. Zhao, W. Y. Ochieng, M. A. Quddus and R. B. Noland: An Extended Kalman Filter Algorithm for Integrating GPS and Low-Cost Dead Reckoning System Data for Vehicle Performance and Emissions Monitoring, *Journal of Navigation*, 2003, 56: 257-275
- [20] S. Leven, J. Zufferey, and D. Floreano: A Minimalist Control Strategy for Small UAVs, in *Proc. IROS*, 2009, pp. 2873-2878
- [21] F. Rovira-Más, R. Banerjee: GPS Data Conditioning for Enhancing Reliability of Automated Off-Road Vehicles. *Proceedings of the Institution of Mechanical Engineers, Part D: Journal of Automobile Engineering*, 2013, 227(4), 521-535
- [22] R. Beard et al: Autonomous Vehicle Technologies for Small Fixed-Wing UAVs, *Journal Of Aerospace Computing Information and Communication* (2005) Volume: 2, Issue: 1, pp. 92-108, ISSN: 19403151
- [23] B. Xiao, K. Zhang, R. Grenfell, T. Norton: Handheld GPS – Today and Tomorrow, *FIG XXII International Congress Washington, D.C. USA*, April 19-26 2002
- [24] A. Molnár, D. Stojcsics: New Approach of the Navigation Control of Small Size UAVs, *Proceedings of 19<sup>th</sup> International Workshop on Robotics in Alpe-Adria-Danube Region*, ISBN: 978-1-4244-6884-3, Budapest, Hungary, 2010, pp. 125-129
- [25] K. Turkoglu, U. Ozdemir, M. Nikbay, E. M. Jafarov: "PID Parameter Optimization of an UAV Longitudinal Flight Control System", *WCSET 2008 World Congress on Science, Engineering and Technology, ICCARV 2008 International Conference on Control, Automation, Robotics and Vision*, 21-23 November 2008, Laval, France
- [26] S. J. Jung, D. Liccardo: Small UAV automation using MEMS, 2007, *IEEE Aerospace and Electronic Systems Magazine*, Vol. 22, No. 5, pp. 30-34
- [27] A. L. Salih, M. Moghavvemi, H. A. F. Mohamed, K. S. Gaeid: Flight PID Controller Design for a UAV Quadrotor, 2010, *Scientific Research and Essays*, Vol. 5, No. 23, pp. 3660-3667
- [28] P. E. I. Pounds, D. R. Bersak, A. M. Dollar: Stability of Small-Scale UAV Helicopters and Quadrotors with Added Payload Mass under PID Control, 2012, *Autonomous Robots*, Vol. 33, No. 1-2, pp. 129-142

- 
- [29] D. Stojcsics, A. Molnar: Fixed-Wing Small-Size UAV Navigation Methods with HIL Simulation for AEROBot Autopilot, Proc. of 9<sup>th</sup> International Symposium on Intelligent Systems and Informatics, Subotica, Serbia, September 8-10, 2011, ISBN: 978-1-4577-1974-5
- [30] A. Cho et al.: Fully Automatic Taxiing, Takeoff and Landing of a UAV using a Single-Antenna GPS Receiver Only, 2007, ICCAS - International Conference on Control, Automation and Systems, p. 821
- [31] B. M. Albaker, N. A. Rahim: Flight Path PID Controller for Propeller-driven Fixed-Wing Unmanned Aerial Vehicles, 2011, International Journal of Physical Sciences, Vol. 6, No. 8, pp. 1947-1964
- [32] A. Molnár: A polgári és katonai robotjárművek fejlesztésében alkalmazott új eljárások és technikai megoldások”, PhD dissertation, 2006, Zrínyi Miklós Nemzetvédelmi Egyetem, Budapest
- [33] D. Stojcsics: Fuzzy Controller for Small Size Unmanned Aerial Vehicles, 10<sup>th</sup> Jubilee International Symposium on Applied Machine Intelligence and Informatics, ISBN: 978-1-4577-0195-5, Herl'any, Slovakia, January 26-28, 2012
- [34] K. M. Passino, S. Yurkovich: Fuzzy Control, Addison Wesley Longman, 1998
- [35] Phoenix Modell: Tiger 60 Instruction manual, Vietnam
- [36] Multiplex GmbH: Xeno building instructions, Germany, 2009